with the use of 10 μl of Lipofectamine reagent (BRL, Gibco) in Dulbecco's modified Eagle's medium (DMEM). The next day the medium was changed to DMEM with serum, and the cells were cultured for 1 day before selection in G418 (400 μg/ml) for 3 to 4 weeks. Purified GSK3β and APC25 were produced as in (*19*). The affinity precipitation of β-catenin from SW 480 cell lysates by purified GSK3β was performed by addition of 2 μg of GSK3β protein to 150 μl of lysate. After a 2-hour incubation at 40°C, the GSK3β was recovered on Glu-Glu antibody coupled to protein G–Sepharose and then analyzed by immunoblotting (*20*).

25. For GSK assays we followed the procedure in (*23*). Immunoprecipitates were prepared for GSK assay by a final wash in kinase assay buffer [25 mM tris (pH 7.5), 5 mM $MgCl_2$, 1 mM dithiothreitol, and 4% glycerol] and then resuspended in 20 μl of buffer containing 50 μM peptide substrate and 50 μM γ-[^{32}P]adenosine triphosphate (ATP) (10,000 cpm/pmol). Assays were performed for 20 min at 30°C, and 10 μl was analyzed for incorporation of ^{32}P. For the phosphorylation of APC in vitro, Glu-Glu–tagged APC25 was produced with the baculovirus-Sf9 cell system (*13*) and then collected from cell lysates on Glu-Glu antibody coupled to protein G–Sepharose. The immobilized APC25 was then dephosphorylated with 4000 units of Lambda phosphatase (New England Biolabs) at 30°C for 2 hours. The dephosphorylated APC25 was eluted from the washed beads with Glu-Glu peptide and then phosphorylated at 30°C in 50 μl of kinase assay buffer containing APC25 (2 to 5 μg) and PKA (2 μg/ml) (Sigma), GSK3β (0.25 μg/ml), or the two kinases added sequentially. For quantitation (Fig. 4A), 50 μM γ-[^{32}P]ATP (10,000 cpm/pmol) was included in the reactions, and radioactive protein was collected by vacuum filtration over nitrocellulose filters. Phosphorylations in Fig. 4B were performed with unlabeled ATP and the phosphoproteins were repurified before being used for affinity precipitation of in vitro–translated β-catenin (wheat germ TNT system, Promega) (*13*).

26. We thank B. Souza and D. Lowe for help with production of recombinant proteins and F. McCormick for critical reading of the manuscript.

15 January 1996; accepted 14 March 1996

Retinal Degeneration in Mice Lacking the γ Subunit of the Rod cGMP Phosphodiesterase

Stephen H. Tsang, Peter Gouras, Clyde K. Yamashita, Hild Kjeldbye, John Fisher,* Debora B. Farber, Stephen P. Goff†

The retinal cyclic guanosine 3′,5′-monophosphate (cGMP) phosphodiesterase (PDE) is a key regulator of phototransduction in the vertebrate visual system. PDE consists of a catalytic core of α and β subunits associated with two inhibitory γ subunits. A gene-targeting approach was used to disrupt the mouse PDEγ gene. This mutation resulted in a rapid retinal degeneration resembling human retinitis pigmentosa. In homozygous mutant mice, reduced rather than increased PDE activity was apparent; the PDEαβ dimer was formed but lacked hydrolytic activity. Thus, the inhibitory γ subunit appears to be necessary for integrity of the photoreceptors and expression of PDE activity in vivo.

Hereditary photoreceptor cell degenerations called retinitis pigmentosa (RP) define a group of genetic diseases causing blindness that affect 1 in 3000 individuals worldwide (*1*). Autosomal dominant, autosomal recessive, sex-linked, and mitochondrial inheritance patterns have been described for RP. A number of mutations affecting the visual pigment rhodopsin (*2*) as well as peripherin/RDS (*3*), a protein of unknown function and localized in the rims of the outer segment discs, result in different forms of dominantly inherited RP (*1*). Most autosomal recessive forms of the disease result from mutations in genes encoding phototransduction proteins (*4*), but the mechanism whereby these mutated genes produce destruction of photoreceptors is not well understood.

Phototransduction begins with the absorption of light by rhodopsin (*5–6*). Photoactivated rhodopsin stimulates the α subunit of a heterotrimeric guanine nucleotide binding protein termed transducin (Tαβγ) to exchange its bound guanosine diphosphate for guanosine triphosphate (GTP) (*7*). The transducin (Tα)-GTP complex dissociates from Tβγ and binds to the inhibitory γ subunits of cyclic guanosine 3′,5′-monophosphate (cGMP) phosphodiesterase ($PDE\alpha\beta\gamma_2$) (*8*). This step removes the constraint that the PDEγ (11 kD) subunit imposes on the catalytic α (88 kD) and β (84 kD) subunits of the heterotetrameric PDE (*7–9*) and increases its hydrolytic activity almost 300-fold (*10*). The activated PDE lowers the intracellular concentration of cGMP (*11*), thereby closing cGMP-gated cation channels on the rod plasma membrane and initiating a neural response to light (*12*). Termination of excitation requires quenching of photoexcited rhodopsin and Tα, deactivation of PDE by reassociation of PDEγ to the PDE αβ catalytic subunits, and restoration of the cGMP concentration through activation of guanylate cyclase. The binding of Tα to PDEγ accelerates the intrinsic guanosine triphosphatase activity of Tα, which also quenches the light response (*10*).

Mutations in the PDEβ subunit gene cause retinal degenerations in both *rd1/rd1* mice (*13*) and Irish Setter dogs (*14*) and are one of the causes of autosomal recessive RP (*15*). Mutations in the PDEα gene can also produce RP (*16*), but no defects have yet been found in the PDEγ gene (*17*). The absence of PDEγ might be expected at least initially to reduce rod cGMP levels by allowing the constitutively uninhibited PDEαβ to hydrolyze cGMP. Consequently, the cGMP-gated cation channels would be permanently closed, eliminating the rod's response to light. To test these notions, we used a gene-targeting approach to generate mice lacking the PDEγ subunit.

Genomic sequences encoding mouse PDEγ were used to construct a targeting DNA (*18*) in which the third exon of the PDEγ gene (*Pdeg*) was replaced with the bacterial neomycin resistance (Neo) gene (Fig. 1A). The mutant allele could not express sequences encoded by the third and fourth exons, including regions required for PDE inhibition (*19*). CCE and R1 embryonic stem (ES) cells (*18*) were transformed with this vector, and G418-gancyclovir–resistant clones were recovered and screened by Southern (DNA) blot analysis. Six independently targeted CCE ES clones were obtained out of 2500 colonies screened, whereas eight mutated clones were recovered from R1 ES cells out of 400 colonies screened. Targeted ES cells were injected into C57BL/6 or MF1 blastocysts that were reimplanted into the uteri of pseudopregnant foster mothers (*20*). The resulting chimeras were bred to generate offspring carrying the mutant allele in the heterozygous form ($Pdeg^{tm1}/+$) in the germ line; intercrosses generated mutant homozygous animals ($Pdeg^{tm1}/Pdeg^{tm1}$) (Fig. 1, B and C). $Pdeg^{tm1}/Pdeg^{tm1}$ homozygous mice were healthy and fertile; thus, PDEγ is not essential for normal prenatal development. Protein immunoblot analysis of a $Pdeg^{tm1}/Pdeg^{tm1}$ retinal homogenate with antisera to either NH_2- or COOH-terminal portions of PDEγ confirmed that the mutant allele did not encode detectable proteins (Fig. 1D). Chimeras were bred with 129/Sv//Ev animals for generation of an inbred line. The $Pdeg^{tm1}/Pdeg^{tm1}$ mice were crossed with MF1, Swiss Webster, and C57BL/6 mice to investigate

S. H. Tsang, J. Fisher, S. P. Goff, Howard Hughes Medical Institute, Department of Biochemistry and Molecular Biophysics, Columbia University, College of Physicians and Surgeons, New York, NY 10032, USA.
P. Gouras and H. Kjeldbye, Edward Harkness Eye Institute, Department of Ophthalmology, Columbia University, College of Physicians and Surgeons, New York, NY 10032, USA.
C. K. Yamashita and D. B. Farber, Jules Stein Eye Institute, Molecular Biology Institute and Department of Ophthalmology, UCLA School of Medicine, Los Angeles, CA 90095, USA.
*Present address: Regeneron Pharmaceuticals, Tarrytown, NY 10591, USA.
†To whom correspondence should be addressed.

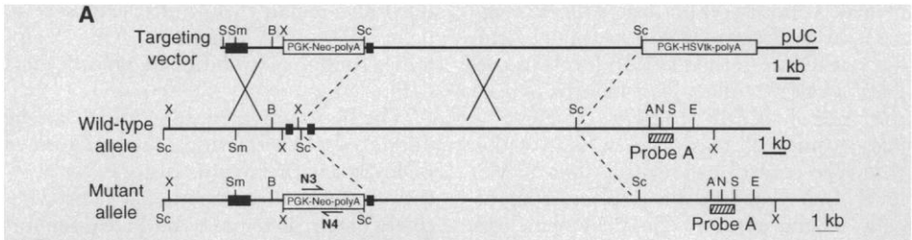

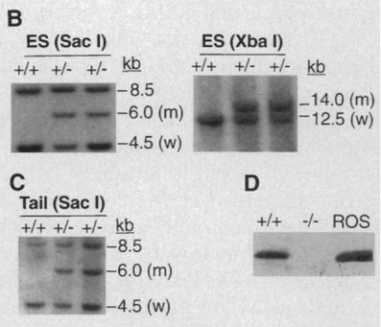

Fig. 1. Targeted disruption of the *Pdeg* gene in ES cells, and germline transmission of the mutant allele. (**A**) Physical map of the targeting vector; the wild-type *Pdeg* locus and the mutant allele are illustrated. The coding exons are indicated by black boxes. Restriction enzyme sites: S, Sal I; Sm, Sma I; B, Bgl II; X, Xba I; Sc, Sac I; A, Acc I; N, Not I; E, Eco RI. N3 and N4 indicate the position of PCR primers. The hatched box shows the position of probe A used to screen for homologous recombination events. (**B**) Southern blot of ES cell DNAs. After Sac I digestion, hybridization with a full-length *Pdeg* cDNA probe (*18*) detects fragments diagnostic of the wild-type (w) allele (4.5 kb) and the targeted (m) allele (6.0 kb). After Xba I digestion, hybridization with probe A detects a wild-type (w) DNA fragment (12.5 kb) and a targeted (m) fragment (14 kb). (**C**) Southern blot with Sac I–digested tail DNA from offspring of a germline chimera, hybridized with *Pdeg* cDNA probe (*18*). (**D**) Protein immunoblot analysis of retinal homogenate (80 μg) from postnatal day 12 $Pdeg^{tm1}/Pdeg^{tm1}$ mutant (−/−) and normal (+/+) offspring obtained from a heterozygote intercross. PDEγ-specific antiserum (HUEY, 1:500 dilution) was used for immunodetection; proteins as small as 3 kD were retained on the blots. Bovine rod outer segment (20 μg) is also shown as a control (ROS).

whether background caused any phenotypic variation; no differences were observed among these backgrounds. *Pdeg* homozygous mutants were also crossed with *rd1* mice to obtain double homozygous mutant mice ($Pdeg^{tm1}/Pdeg^{tm1}$ *rd1/rd1*) lacking both PDEγ and PDEβ subunits.

Heterozygous animals were histologically and physiologically normal, demonstrating that the $Pdeg^{tm1}$ allele is genetically recessive. Examination of the retinal physiology (*21*) of the homozygous mutants, however, revealed a profound photoreceptor abnormality. Compared to wild-type (+/+) or heterozygous ($Pdeg^{tm1}/+$) controls, the electroretinogram (ERG) of $Pdeg^{tm1}/Pdeg^{tm1}$ mice showed a severely diminished response in both a- and b-wave components, with a delay in b-wave implicit time. Both of these changes are characteristic of human RP (Fig. 2A). The loss in response was much greater in 8-week-old than in 2-week-old animals (Fig. 2A). The ERG became almost undetectable after 3 months. Thus, the targeted mutation resulted in a progressive loss of photoreceptor function (Fig. 2B). Indistinguishable ERG measurements were also found in the PDEβ-deficient (*rd1/rd1*) and

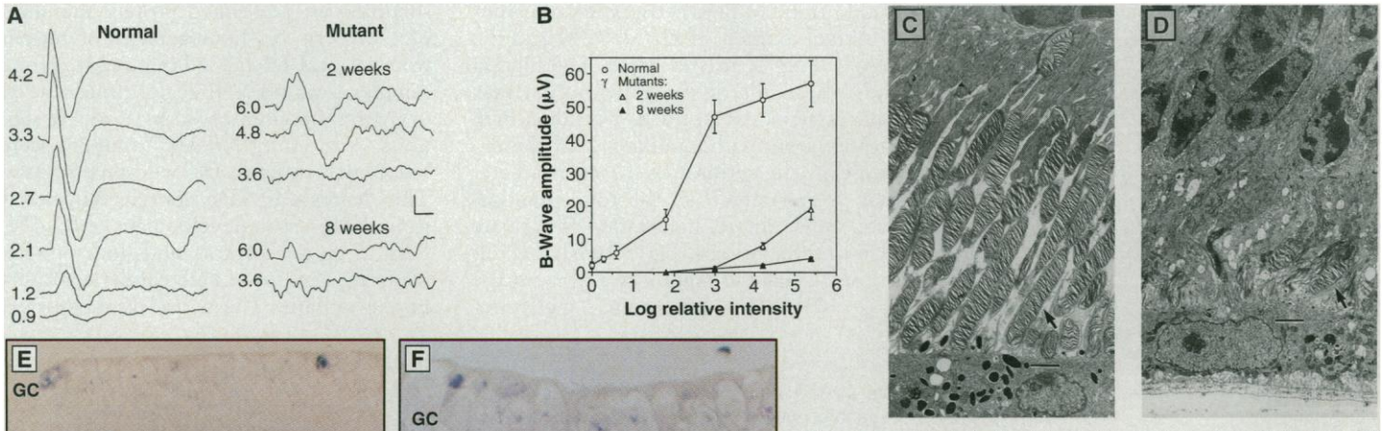

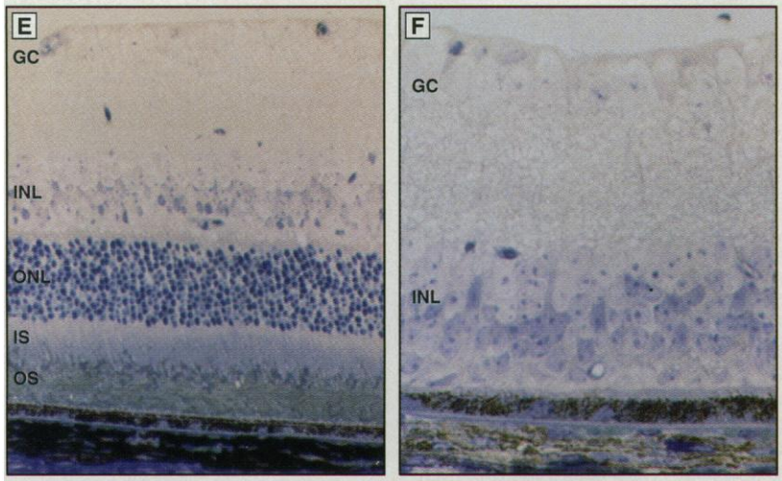

Fig. 2. Physiological and morphological characterization of $Pdeg^{tm1}/Pdeg^{tm1}$ homozygous mutant mice. (**A**) Corneal ERGs of a normal mouse (left) compared to those of a mutant mouse (right) at 2 and 8 weeks after birth. Each trace is 0.7 s in duration and represents the average of 100 responses of a 1-Hz square-wave flickering stimulus of equal duty cycle. The numbers on the left indicate the log relative energy of the light stimulus. Corneal positivity is shown as an upward deflection. Vertical calibration: 25 μV for the upper trace, 12 μV for the second and third traces, 8 μV for the fourth trace, and 6 μV for the lower two traces on the left and all the traces on the right; horizontal calibration: 75 ms for all traces. (**B**) The relation between the amplitude of the b-wave of the ERG (ordinate) in microvolts and the light intensity of the stimulus (abscissa) in relative logarithmic units for normal (○) and $Pdeg^{tm1}/Pdeg^{tm1}$ mutants at 2 (△) and 8 (▲) weeks of age. Each point represents the mean (±SE) of 27 mice for the normal function, 39 mice for the 8 week function, and 6 mice for the 2 week function. (**C** and **D**) Transmission electron micrographs of the photoreceptor layer (bar, 2 μm) of 13-day-old control mouse (C) and $Pdeg^{tm1}/Pdeg^{tm1}$ mutant mouse (D). The outer segments (indicated by an arrow) of $Pdeg^{tm1}/Pdeg^{tm1}$ mutants became disorganized and shortened at this age compared with wild-type mice. (**E** and **F**) Light micrograph of the retina from 8-week-old control mouse (E) and $Pdeg^{tm1}/Pdeg^{tm1}$ mutant mouse (F). OS, outer segments; IS, inner segments; ONL, outer nuclear layer; INL, inner nuclear layer; GC, ganglion cell layer. The retina of the $Pdeg^{tm1}/Pdeg^{tm1}$ mutant mouse (F) has lost the photoreceptor layer (OS, IS, ONL) completely by 8 weeks of age. The inner nuclear and ganglion cell layers (F) appear to be unaffected in the $Pdeg^{tm1}/Pdeg^{tm1}$ mouse.

the PDEβ-PDEγ–deficient (*Pdeg*^{tm1}/*Pdeg*^{tm1} *rd1*/*rd1*) mice (*22*).

Retinas of *Pdeg*^{tm1}/*Pdeg*^{tm1} mice of different ages were examined histologically (*23*). Transmission electron microscopy revealed that the photoreceptor outer segments had failed to develop normally and were disorganized at postnatal day 10 (P10), and that most of the outer segments were lost by P13, although the photoreceptor nuclear layer remained intact (Fig. 2, C and D). Subsequently, from P14 to P21, a progressive loss of photoreceptor nuclei was observed that was more severe in the central relative to the peripheral portion of the retina. Only a single row of photoreceptor nuclei remained by 3 weeks of age, and the retina was completely devoid of a photoreceptor layer by 8 weeks (Fig. 2, E and F). Similar progression of retinal degeneration was seen in *rd1*/*rd1* and *Pdeg*^{tm1}/*Pdeg*^{tm1} *rd1*/*rd1* mice.

The levels of cGMP present in homogenates of the posterior pole were assayed at various times during development (*24*). Surprisingly, levels of cGMP were increased in the *Pdeg*^{tm1}/*Pdeg*^{tm1} retinas. These levels peaked at P16 (67.7 pmol mg^{-1} protein) and were fivefold greater than those in wild-type (+/+) mice of comparable age (13.3 pmol mg^{-1} protein). Moreover, the increase in cGMP levels preceded photoreceptor degeneration (Fig. 3A). In contrast to wild-type mice, light did not reduce retinal cGMP levels in the *Pdeg*^{tm1}/*Pdeg*^{tm1} mice. By 3 months of age, the retinal cGMP content of *Pdeg*^{tm1}/*Pdeg*^{tm1} mice decreased below that of the wild-type controls, indicating that cGMP levels were primarily due to photoreceptor cells of the retina. The developmental pattern of retinal cGMP levels for *Pdeg*^{tm1}/*Pdeg*^{tm1} mice was not substantially different from that of *rd1*/*rd1* or the *Pdeg*^{tm1}/*Pdeg*^{tm1} *rd1*/*rd1* mice (*22*).

These results suggest that the loss of the PDEγ subunit caused a defect in the enzymes involved in retinal cGMP metabolism. Increased cGMP levels in *Pdeg*^{tm1}/*Pdeg*^{tm1} retinas could be the result of either an increased guanylate cyclase activity or a defective PDE activity. Measurement of retinal guanylate cyclase activity showed virtually no difference between control (12.2 ± 0.6 nmol min^{-1} mg^{-1} protein) and *Pdeg*^{tm1}/*Pdeg*^{tm1} (12.4 ± 0.8 nmol min^{-1} mg^{-1} protein) mice at P12, indicating normal cyclase function. Retinal PDE activity in *Pdeg*^{tm1}/*Pdeg*^{tm1} mice (*25*), however, was well below the levels detected in wild-type mice during the course of photoreceptor development (Fig. 3B). A similar trend of PDE activity was apparent in retinal extracts of *rd1*/*rd1* (*25*) and the *Pdeg*^{tm1}/*Pdeg*^{tm1} *rd1*/*rd1* mice. The bipolar and other cells of the inner retina may have contributed to the low residual PDE activity seen in the mutants, and the decrease in the retina may be even greater than is apparent from the total homogenate. Furthermore, light failed to activate PDE in these retinas (Fig. 3B); basal levels in the 12-day-old mutant were low in the dark (10.9 ± 1.41 nmol min^{-1} mg^{-1} protein) and remained low after exposure to light (10.0 ± 3.6 nmol min^{-1} mg^{-1} protein), similar to findings in *rd1*/*rd1* mice (*25*).

The light-activated state of PDE can be mimicked by treating the preformed PDE$\alpha\beta\gamma_2$ with trypsin, histone, or polycations such as protamine, which selectively digest or remove the PDEγ subunit (*11*). The kinetics of PDE activation in vitro correspond to the degradation of PDEγ by trypsin (*26*). Homogenates were prepared from P12 retinas of mutant and control animals and assayed for PDE after various treatments. Trypsinization markedly increased PDE activity in wild-type mice (from a basal level of 27.7 ± 2.5 to 2059 ± 225 nmol min^{-1} mg^{-1} protein). No significant activation by trypsin was observed in comparable *Pdeg*^{tm1}/*Pdeg*^{tm1} mice (increase from 10.9 ± 1.4 to only 15.7 ± 2.2 nmol min^{-1} mg^{-1} protein).

The low PDE activity measured in the mutant mice retinas suggested that the loss of the inhibitory γ subunit might have caused either a quantitative change in the level of PDEα and PDEβ or an alteration in the hydrolytic activity of the PDEα/β complex. To determine whether there was a decrease in the amount of PDE α and β subunits, we performed protein immunoblot analysis on homogenates of retinas from 12- and 13-day-old mice (*27*). When samples were normalized for protein (Fig. 4A), the amounts of both α and β subunits in the *Pdeg*^{tm1}/*Pdeg*^{tm1} mutant were one-fourth those in the wild-type retinas. This decrease in PDE content may result from the arrest in development of *Pdeg*^{tm1}/*Pdeg*^{tm1} photoreceptors and does not account for the loss of PDE catalytic activity in the mutant. The α and β subunits of

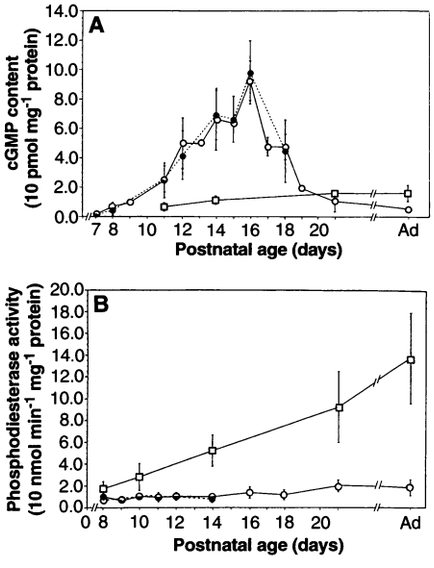

Fig. 3. Developmental cGMP content and PDE activity in the retinas of control and mutant mice. (**A**) cGMP content in the freshly dissected posterior poles of *Pdeg*^{tm1}/*Pdeg*^{tm1} and wild-type animals during postnatal development (*22*). The results indicated are means ± SEM of three to nine samples. (**B**) PDE activity in freshly dissected retinas of *Pdeg*^{tm1}/*Pdeg*^{tm1} mutant and wild-type mice (*23*). The results indicated are means ± SEM of three to nine samples. Light- (○) or dark-adapted (●) *Pdeg*^{tm1}/*Pdeg*^{tm1} mutant retinas and light-adapted control retinas (□) are indicated.

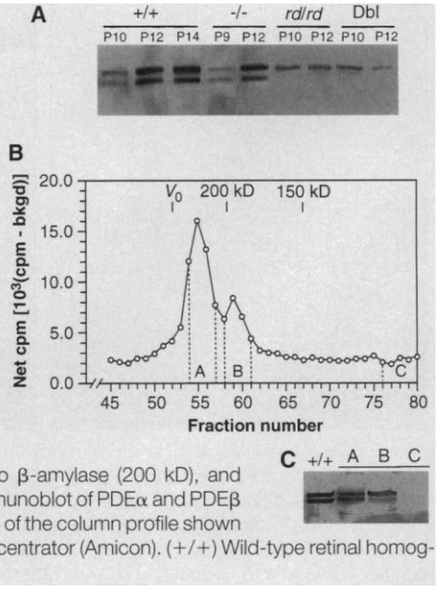

Fig. 4. Analysis of PDEα and PDEβ subunits in mutant retinal homogenates. (**A**) Protein immunoblot of PDEα and PDEβ subunits. Proteins from retinal homogenate (80 μg) were separated by SDS-PAGE, transferred to nitrocellulose, and immunoblotted with MOE polyclonal antibody to PDE (1:2000 dilution). (+/+) Wild type; (−/−) *Pdeg*^{tm1}/*Pdeg*^{tm1} mice; *rd/rd*, *rd1*/*rd1* mutants; Dbl, double homozygous *Pdeg*^{tm1}/*Pdeg*^{tm1} *rd1*/*rd1* mice. The upper band of the doublet is PDEα and the lower band is PDEβ. (**B**) Elution profile of PDE activity from an extract of 20 retinas of *Pdeg*^{tm1}/*Pdeg*^{tm1} mutants at postnatal day 12. The sample was loaded on Sephacryl S-200 HR column (1.5 by 100 cm) and eluted at 6 ml/hour with 1.0-ml fractions collected. Fractions were assayed for PDE activity (*23*) in the presence of 50 μM cGMP, and total cpm minus background was plotted versus fraction number. The column was calibrated with dextran blue 2000 (V_0), sweet potato β-amylase (200 kD), and yeast alcohol dehydrogenase (150 kD). (**C**) Protein immunoblot of PDEα and PDEβ subunits in fractions pooled from the indicated regions of the column profile shown in (B) and concentrated on a Centricon-100 microconcentrator (Amicon). (+/+) Wild-type retinal homogenate (30 μg).

PDE were not detected in adult $Pdeg^{tm1}/Pdeg^{tm1}$ mutant mice because of the loss of the photoreceptor cell layer. Furthermore, the PDEβ subunit was always absent in *rd1/rd1* or $Pdeg^{tm1}/Pdeg^{tm1}$ *rd1/rd1* double homozygous animals (Fig. 4A).

To determine whether the two PDE catalytic subunits from the $Pdeg^{tm1}/Pdeg^{tm1}$ mutant mice were present in a native conformation, we subjected homogenates to size exclusion chromatography on a Sepharose S200 column, and fractions were collected and analyzed for PDE activity and for the presence of α and β subunits by SDS–polyacrylamide gel electrophoresis (PAGE) and protein immunoblotting (Figs. 4, B and C). The main peak of activity, eluting at an apparent molecular size of ~220 to 230 kD, contained comparable amounts of α and β subunits. This peak may also have contained the δ subunits of PDE (*28*). A smaller peak, eluting at about 180 to 190 kD, contained both α and β subunits and may represent just the catalytic core (Fig. 4B). Similar profiles were obtained with wild-type retinal homogenates. Examination of fractions eluted at the position expected for monomeric α or β subunits by protein immunoblotting did not reveal detectable amounts of these proteins (*27*). Thus, loss of PDEγ did not affect the apparent size of the enzyme, nor did it seem to alter the assembly of the PDE catalytic core into a dimer. The presence of the two PDE subunits in $Pdeg^{tm1}/Pdeg^{tm1}$ mice distinguishes this mutant phenotype from that of the *rd1/rd1* mice.

Our results indicate that an interaction between the γ subunit and PDEαβ is essential for the proper activation of PDE and that all three subunits may be essential for assembly of a stable, active holoenzyme. It is also possible that other proteins normally involved in light adaptation, including transducin α (*29*), may inhibit PDE in the absence of the γ subunit. In either case, the genetic loss of PDEγ is manifested as an increase in cGMP content in the developing mutant retinas. Thus, the $Pdeg^{tm1}/Pdeg^{tm1}$ mice effectively recapitulate the defect seen in the *rd1/rd1* mouse and may suffer retinal degeneration through a similar mechanism. The high cGMP concentrations may keep cGMP-gated cationic channels open continuously and lead to an excessive energy load on the rod photoreceptors, resulting in degeneration.

REFERENCES AND NOTES

1. P. Humphries, P. Kenna, G. J. Farrar, *Science* **256**, 804 (1992).
2. T. P. Dryja *et al.*, *Nature* **343**, 364 (1990); C. H. Sung *et al.*, *Proc. Natl. Acad. Sci. U.S.A.* **88**, 6481 (1991); V. C. Sheffield, G. A. Fishman, J. S. Beck, A. E. Kimura, E. M. Stone, *Am. J. Hum. Genet.* **49**, 699 (1991).
3. G. Connell *et al.*, *Proc. Natl. Acad. Sci. U.S.A.* **88**, 723 (1991); G. J. Farrar *et al.*, *Nature* **354**, 478 (1991); K. Kajiwara *et al.*, *ibid.*, p. 480; G. H. Travis, J. G. Sutcliffe, D. Bok, *Neuron* **6**, 61 (1991).
4. T. P. Dryja *et al.*, *Proc. Natl. Acad. Sci. U.S.A.* **92**, 10177 (1995); R. R. McInnes and R. A. Bascom, *Nature Genet.* **1**, 155 (1992).
5. H. Kuhn and P. A. Hargrave, *Biochemistry* **20**, 2410 (1981).
6. L. Stryer, *J. Biol. Chem.* **266**, 10711 (1991); S. Yarfitz and J. B. Hurley, *ibid.* **269**, 14329 (1994).
7. B. K.-K. Fung, J. B. Hurley, L. Stryer, *Proc. Natl. Acad. Sci. U.S.A.* **78**, 152 (1981).
8. A. Sitaramayya, J. Harkness, J. H. Parkes, C. Gonzalez-Oliva, P. A. Liebman, *Biochemistry* **25**, 651 (1986); T. G. Wensel and L. Stryer, *Proteins Struct. Funct. Genet.* **1**, 90 (1986).
9. W. Baehr, M. J. Devlin, M. L. Applebury, *J. Biol. Chem.* **254**, 11669 (1979); B. K.-K. Fung, J. H. Young, H. K. Yamane, I. Griswold-Prenner, *Biochemistry* **29**, 2657 (1990); P. Deterre, J. Bigay, F. Forquet, M. Robert, M. Charbre, *Proc. Natl. Acad. Sci. U.S.A.* **85**, 2424 (1988).
10. V. Y. Arshavsky and D. M. Bownds, *Nature* **357**, 416 (1992).
11. N. Miki, J. M. Baraban, J. J. Keins, J. J. Boyce, M. W. Bitensky, *J. Biol. Chem.* **260**, 6320 (1975).
12. K.-W. Yau, *Invest. Ophthalmol. Vis. Sci.* **35**, 9 (1994).
13. C. Bowes *et al.*, *Nature* **347**, 677 (1990); S. J. Pittler and W. Baehr, *Proc. Natl. Acad. Sci. U.S.A.* **88**, 8322 (1991); C. Bowes *et al.*, *ibid.* **90**, 2955 (1993).
14. D. B. Farber, J. Danciger, G. Aguirre, *Neuron* **9**, 349 (1992); M. L. Suber *et al.*, *Proc. Natl. Acad. Sci. U.S.A.* **90**, 3968 (1993); K. Ray, V. J. Baldwin, G. M. Acland, S. H. Blanton, G. D. Aguirre, *Invest. Ophthalmol. Vis. Sci.* **35**, 4291 (1994).
15. M. E. McLaughlin, T. L. Ehrhart, E. L. Berson, T. P. Dryja, *Proc. Natl. Acad. Sci. U.S.A.* **92**, 3249 (1995); M. Bayes *et al.*, *Hum. Mutation* **5**, 228 (1995); M. Danciger *et al.*, *Genomics* **3**, 1 (1995).
16. S. H. Huang *et al.*, *Invest. Ophthalmol. Vis. Sci.* **36**, S825 (1995).
17. L. B. Hanh, E. L. Berson, T. P. Dryja, *ibid.* **35**, 1077 (1994).
18. A 0.48-kb *Pdeg* complementary DNA (cDNA) fragment [N. Tuteja and D. B. Farber, *FEBS Lett.* **232**, 182 (1988)] was used to isolate a 16-kb genomic DNA from a mouse λ FixII 129/SvJ library. A targeting vector was constructed by insertion of a 2.0-kb fragment containing exon 2 on the 5′ side, and an 8.5-kb fragment containing exon 4 on the 3′ side, of the neomycin casette of plasmid pPNT (provided by R. Mulligan). DNA was linearized with Sal I before use for electroporation into ES cells. The CCE (provided by E. J. Robertson) and R1 (provided by V. E. Papaioannou, A. Nagy, R. Nagy, W. Abramow-Newerly, J. Roder, and J. Rossant) [A. Nagy, J. Rossant, R. Nagy, W. Abramow-Newerly, J. C. Roder, *Proc. Natl. Acad. Sci. U.S.A.* **90**, 8424 (1993)] ES cells were cultured, electroporated with the Ω-replacement targeting vector, selected, and screened [P. L. Schwartzberg, S. P. Goff, E. J. Robertson, *Science* **246**, 799 (1989)]. Homologous recombination at the *Pdeg* locus was further confirmed by digestion of the targeted clones with various enzymes that did not cut the targeting vector.
19. N. P. Skiba, N. O. Artemyev, H. E. Hamm, *J. Biol. Chem.* **270**, 13210 (1995); D. J. Takemoto, D. Hurt, B. Oppert, J. Cunnick, *Biochem. J.* **281**, 637 (1992); V. M. Lipkin, I. L. Dumler, K. G. Muradov, N. O. Artemyev, R. N. Etingof, *FEBS. Lett.* **234**, 287 (1988).
20. The targeted mutation at the *Pdeg* locus was introduced into the germ line of chimeric mice by injection of the targeted ES clones into C57BL/6 or MF1 blastocysts that were surgically reimplanted into the uteri of foster mothers [V. E. Papaioannou and R. Johnson, in *Gene Targeting*, A. L. Joyner, Ed. (Oxford Univ. Press, New York, 1993), pp. 107–146; A. Bradley, in *Teratocarcinomas and Embryonic Stem Cells: A Practical Approach*, E. J. Robertson, Ed. (IRL, Oxford, 1987), pp. 113–151]. Thirty-six chimeras were born and mated with C57BL/6 or MF1 mice to test for germline competency of the targeted clones; 29 of these chimeric mice transmitted the mutant allele. ES cell–derived progeny were identified by coat color and screened for the presence of the targeted allele by Southern blot or polymerase chain reaction (PCR) analysis or both. The primers used were N3 and N4 (Fig. 1A) and 3.0 and 3.2 (within the deleted third exon): N3: 5′-AGAGGCTATTCGGCTATGACTG-3′; N4: 5′-CCTGATCGACAAGACCGGCTTC-3′; 3.0: 5′-CTGGAATGGAAGGCCTGGG-3′; and 3.2: 5′-TGGTGAACCTACCCATGGGG-3′. The N3 and N4 primer pair amplified a 400–base pair (bp) fragment from the mutant locus, and the 3.0 and 3.2 primer pair amplified a 200-bp fragment from the wild-type locus. $Pdeg^{tm1}$ mice were all screened against the presence of the *rd1* genotype as described (*13*).
21. ERGs were obtained from anesthetized mice with a AgCl saline cotton wick electrode contacting the cornea [S. Yamamoto, J. Du, P. Gouras, H. Kjeldbye, *Invest. Ophthalmol. Vis. Sci.* **34**, 3068 (1993)]. The light source was a helium-neon laser (544 nm) led through a fiber optic bundle 6 mm in diameter directly before the diad pupil. We used two methods of stimulation: a light chopper that produced flickering square-wave stimuli at 1 Hz, which were averaged by a computer; or a Vincent shutter to obtain 0.1-s pulses that were repeated every 5 to 10 s at high stimulus intensities. The maximal responses at 2 to 3 weeks after birth were 600 to 800 μV from normal mice but only 20 to 30 μV from mutants.
22. S. H. Tsang *et al.*, unpublished data.
23. Retinas were fixed by vascular perfusion of the mice with a solution of 3% glutaraldehyde and 1.5% paraformaldehyde in phosphate-buffered saline at pH 7.2. Epon-embedded blocks were prepared as described [P. Gouras, J. Du, H. Kjeldbye, S. Yamamoto, D. Zack, *Invest. Ophthalmol. Vis. Sci.* **35**, 3145 (1994)]. Single sections of the retina extending from the ora serrata superiorally to the ora serrata inferiorally, including the optic nerve, were examined by light microscopy; selected areas were also studied by electron microscopy.
24. The assay was done essentially as described [D. B. Farber and R. N. Lolley, *Science* **186**, 449 (1974)], except that the posterior pole of the globe was dissected and homogenized in 0.1N HCl.
25. To minimize individual differences between mice, we pooled retinas of two or more mice for each time point assayed. Each reaction was done in triplicate. Cyclase and PDE assays were done essentially as described [D. B. Farber and R. N. Lolley, *J. Cyclic Nucleotide Res.* **2**, 139 (1976)]. Cyclase assays contained EGTA. PDE assays were done with 300,000 dpm [^{3}H]cGMP and 250 μM cGMP in 40 mM tris (pH 7.5), 5 mM $MgCl_2$, and 1 mM dithiothreitol. The protein content of each homogenate was determined by standard Lowry assays.
26. J. B. Hurley and L. Stryer, *J. Biol. Chem.* **257**, 11094 (1982).
27. Proteins from retinal homogenates were separated by SDS-PAGE with a tris-tricine buffer system and an inverted acrylamide gradient [R. Zardoya *et al.*, *Biotechniques* **16**, 271 (1994)]. Proteins were blotted and probed with MOE, DUEY, or HUEY antiserum and developed with the amplified alkaline phosphatase kit (Bio-Rad).
28. G. Gillespie, R. K. Prusti, E. D. Apel, J. A. Beavo, *J. Biol. Chem.* **264**, 12187 (1989).
29. S. Kroll, W. J. Phillips, R. A. Cerione, *ibid.*, p. 4490.

30. We thank R. Axel, F. Costantini, B. K.-K. Fung, J. L. German III, P. Mombaerts, A. Nagy, V. E. Papaioannou, J. Rossant, A. Tomlinson, D. Warburton, and members of their laboratories for sharing ideas, cell lines, antisera, and equipment, and for critically reading the manuscript; E. Carlson, C.-S. Lin, M. Mendelsohn, and F. Wang for guidance and advice; and members of the Farber, Goff, and Gouras laboratories for support, especially W. Li. S.H.T. is supported by Medical Scientist Training Program fellowship T32 GM 073667-14. Supported by NIH grants EY08285 (D.B.F.) and by grants from the George Gund Foundation and the Foundation Fighting Blindness (D.B.F.). D.B.F. is the recipient of a Senior Scientific Investigator Award from Research to Prevent Blindness. S.P.G. is an Investigator of the Howard Hughes Medical Institute.

4 January 1996; accepted 13 March 1996